Theory of the de Haas–van Alphen Effect in a System of Coupled Orbits. Application to Magnesium*

L. M. Falicov† and Henryk Stachowiak‡

Department of Physics and Institute for the Study of Metals, University of Chicago, Chicago, Illinois

(Received 23 February 1966)

A Green's-function formulation for the calculation of amplitudes of the de Haas-van Alphen effect is developed. The theory can be applied to the case of metals in which magnetic breakdown takes place. The exact theory is presented and then approximated by a wave-packet approach susceptible of a simple physical interpretation; this approximation is proved to involve no error for the free-electron gas. The method is then applied to a hexagonal network corresponding to the case of magnesium for magnetic fields parallel to the hexad axis. Curves are presented for the magnetic-field dependence of the amplitude of various important periods at $T = 1°K$; they are in agreement with preliminary experimental data. The method is also proved to give a density of states which agrees with that obtained from Pippard's model for the hexagonal network of coupled orbits.

1. INTRODUCTION

THE de Haas–van Alphen effect has proved to be an extremely useful tool for investigating the electronic properties of metals and semi-metals.[1] At low temperatures the magnetization exhibits oscillations periodic in H^{-1} whose frequencies ν are directly proportional to extremal cross-sectional areas α_0 of the Fermi surface, i.e.,

$$\nu = \frac{hc\alpha_0}{2\pi e}; \quad \alpha_0(\text{a.u.}) = 2.673 \times 10^{-9}\nu(\text{G}). \quad (1.1)$$

Consequently, measurements of the de Haas–van Alphen frequencies give direct and detailed information on the electronic structure. The amplitude of the oscillations on the other hand is a much more complex quantity to analyze and many factors are known to contribute: the curvature of the Fermi surface at the extremum, the temperature, the mean free path of the electrons, and the spin-orbit coupling among others. The functional dependences of the amplitude on the temperature and on magnetic field strength are, however, in most cases practically identical to that found theoretically for the free-electron case.[2] This means that the free energy of the system shows a dependence of the form

$$F \propto H^{5/2}\frac{X}{\sinh X}\cos\left(\frac{hc\alpha_0}{eH} - \varphi_0\right) \quad (1.2)$$

for each extremal cross-sectional area α_0 of the Fermi surface (or their multiples). In (1.2)

$$X = \frac{2\pi^2 k_B T}{\hbar\omega_c}, \quad (1.3)$$

ω_c is the cyclotron frequency corresponding to the area α_0, and φ_0 is an arbitrary phase.

Some metals however, Zn in particular,[3] are known experimentally to follow a different behavior, namely a much slower increase or even a decrease in the amplitude of some oscillations as the magnetic field increases. This behavior can be explained qualitatively in terms of magnetic breakdown, a phenomenon which in the last five years has received considerable attention from the theoretical[4–11] as well as the experimental[11–17] point of view. Nonetheless, no complete theory of the de Haas–van Alphen effect in metals with magnetic breakdown has been presented so far, and, although the value of the frequencies can be easily

[1] See, for example, D. Shoenberg, in *Progress in Low Temperature Physics*, edited by C. J. Gorter (North-Holland Publishing Company, Amsterdam, Netherlands, 1957), Vol. 2, p. 226; D. Shoenberg, in *The Fermi Surface*, edited by W. A. Harrison and M. B. Webb (John Wiley & Sons, Inc., New York, 1960), p. 74; A. B. Pippard, Repts. Progr. Phys. 23, 176 (1960); and the many references quoted there.

[2] R. E. Peierls, *Quantum Theory of Solids* (Clarendon Press, Oxford, England, 1955), p. 144 ff.

[3] J. S. Dhillon and D. Shoenberg, Phil. Trans. Roy. Soc. (London) A248, 1 (1955).

[4] M. H. Cohen and L. M. Falicov, Phys. Rev. Letters 7, 231 (1961).

[5] E. I. Blount, Phys. Rev. 126, 1636 (1962).

[6] A. B. Pippard, Proc. Roy. Soc. (London) A270, 1 (1962).

[7] A. B. Pippard, Phil. Trans. Roy. Soc. (London) A256, 317 (1964).

[8] E. Brown, Phys. Rev. 133, A1038 (1964).

[9] W. G. Chambers, Phys. Rev. 140, A135 (1965).

[10] L. M. Falicov and P. R. Sievert, Phys. Rev. Letters 12, 550 (1964); Phys. Rev. 138, A88 (1965); L. M. Falicov, A. B. Pippard, and P. R. Sievert (to be published).

[11] M. G. Priestley, L. M. Falicov, and G. Weisz, Phys. Rev. 131, 617 (1963).

[12] M. G. Priestley, Proc. Roy. Soc. (London) A276, 258 (1963).

[13] R. W. Stark, T. G. Eck, and W. L. Gordon, Phys. Rev. 133, A443 (1964).

[14] R. W. Stark, Phys. Rev. Letters 9, 482 (1962); Phys. Rev. 135, A1698 (1964).

[15] R. W. Stark, in *Proceedings of the IXth International Conference on Low Temperature Physics, Columbus, Ohio, 1964* (Plenum Press, New York, 1965), p. 712.

[16] A. C. Thorsen, L. E. Valby, and A. S. Joseph, in *Proceedings of the IXth International Conference on Low Temperature Physics, Columbus, Ohio, 1964* (Plenum Press, New York, 1965), p. 867.

[17] M. G. Priestley and R. W. Stark (private communication and to be published).

understood from the basic properties of the magnetic-breakdown phenomenon, the amplitude of the oscillations and particularly its magnetic-field dependence need further examination.

Two recent developments motivate our study. Firstly, new and detailed experiments[17] on the de Haas-van Alphen effect in magnesium show such a wealth of information that a theory of the effect becomes a necessity if one is to interpret the data correctly. Secondly, the quantum mechanical properties of electrons in a system of coupled orbits[6,7,9] have been exhaustively studied and an extension to include the theory of the de Haas-van Alphen effect became thus possible.

In Sec. 2 we present a theoretical formulation of the problem by developing an exact Green's function or wave-packet approach. The exact theory is then approximated by introducing some simplifying assumptions. The method is tested by performing the calculation for the simple cases of the free-electron gas[2] and the free-electron gas with scattering included,[18] and comparing our results with the well-known ones for these examples.

In Sec. 3 the method is applied to the case of magnetic breakdown, i.e., the case in which orbits are coupled. In Sec. 4 the specific case of magnesium is studied and a calculation of the relative amplitude of various important de Haas-van Alphen periods is carried out. The method is tested again by comparing the resulting density of states with a numerical calculation of the density of states corresponding to the specific band structure computed by Pippard.[7]

2. FORMULATION OF THE THEORY

In calculations of the de Haas-van Alphen effect, the magnetization of the metal is calculated by the standard formula

$$M(H) = -\frac{\partial F}{\partial H};\qquad (2.1)$$

the free energy F is in turn given by[2]

$$F = N\zeta - 2k_BT \int \rho(E,H)$$

$$\times \ln\{1 + \exp[(\zeta - E)/k_BT]\}dE, \quad (2.2a)$$

or equivalently, if an integration by parts is carried on in (2.2a), by

$$F = N\zeta - 2\int f(E,T)\int^E \rho(E',H)dE'dE. \quad (2.2b)$$

In (2.2) ζ is the Fermi energy, $f(E,T)$ the Fermi-Dirac distribution function and $\rho(E,H)$ the magnetic-field-

[18] R. B. Dingle, Proc. Roy. Soc. (London) **A211**, 500, 517 (1952).

dependent density of states. The major task in the calculation is thus the determination of $\rho(E,H)$.

In order to calculate $\rho(E,H)$ we introduce now a Green's function $G(\mathbf{r},\mathbf{r}_0,t)$ which satisfies Schrödinger's equation

$$i\hbar\frac{\partial}{\partial t}G(\mathbf{r},\mathbf{r}_0,t) = \mathcal{3C}G(\mathbf{r},\mathbf{r}_0,t) \qquad (2.3)$$

subject to the initial condition

$$G(\mathbf{r},\mathbf{r}_0,0) = \delta(\mathbf{r}-\mathbf{r}_0). \qquad (2.4)$$

In (2.3) $\mathcal{3C}$ is the one-electron Hamiltonian of the crystal, acting on the variable $\mathbf{r}$. It is easy to prove (see Appendix A) by expansion of G in the eigenfunctions of $\mathcal{3C}$, that

$$\rho(E) = \frac{1}{2\pi\hbar}\int\int G(\mathbf{r}_0,\mathbf{r}_0,t)\exp[iEt/\hbar]d\mathbf{r}_0dt. \quad (2.5)$$

Consequently, the knowledge of $G(\mathbf{r}_0,\mathbf{r}_0,t)$ is equivalent to the knowledge of the density of states $\rho(E)$ since one essentially is the Fourier transform of the other.

Equations (2.3)–(2.5) are susceptible of very physical interpretation: $G(\mathbf{r},\mathbf{r}_0,t)$ describes the evolution of a wave packet which at $t=0$ is perfectly localized at $\mathbf{r}=\mathbf{r}_0$. As time evolves (both in the positive as well as the negative directions) the wave packet spreads out. The amplitude and phase of this wave-packet at every instant of time at the point of initial localization $\mathbf{r}_0$, integrated over all values of $\mathbf{r}_0$, give the Fourier transform of the density of states; that is, we should focus our attention to those parts of the wave packet that stay localized at $\mathbf{r}_0$ or return to $\mathbf{r}_0$ after a given interval of time.

In order to gain further insight into the properties of G, we calculate it for two simple cases: (a) a two-dimensional field-free electron gas, and (b) a two-dimensional free-electron gas in the presence of a magnetic field. The usefulness for our purposes of the two-dimensional (rather than three-dimensional) problems will be apparent later. We shall assume that the two-dimensional electron gas is confined to an area L_1L_2 and that all energies are measured with respect to the Fermi energy, assumed to be a constant independent of magnetic fields.

(a) Two-Dimensional Field-Free Electron Gas

Since the eigenfunctions are plane waves, Eq. (A2) in Appendix A immediately yields

$$G(\mathbf{r}_0,\mathbf{r}_0,t) = \frac{2}{L_1L_2}\sum_k \exp[-i\hbar(k^2 - k_F^2)t/2m]$$

$$= \frac{2m}{\hbar}\exp[i\hbar k_F^2t/2m]\delta_+(t). \qquad (2.6)$$

In (2.6) k_F is the Fermi wave vector,

$$\delta_+(x) = \tfrac{1}{2}\delta(x) + \frac{1}{2\pi i}\frac{\mathcal{P}}{x},\qquad (2.7)$$

and the factor of 2 is due to spin degeneracy. Insertion of (2.6) into (2.5) yields the expected result

$$\rho(E) = \frac{m}{\pi\hbar^2}L_1L_2,\quad E > -\frac{\hbar^2k_F{}^2}{2m};$$

$$= 0,\qquad E < -\frac{\hbar^2k_F{}^2}{2m}. \qquad (2.8)$$

It can be seen that the appearance in (2.6) of a δ_+ function rather than a simple Dirac δ function guarantees that $\rho(E)$ is zero for energy values below the bottom of the band $E_o = -E_F = -\hbar^2k_F{}^2/2m$; this insures convergence in the lower limit of all integrals involving $\rho(E)$.

(b) Two-Dimensional Free-Electron Gas in the Presence of a Magnetic Field

The derivation for this case is given in detail in Appendix B. It is shown there [Eq. (B5)] that $G(\mathbf{r}_0,\mathbf{r}_0,t)$ consists of a series of δ_+ functions with arguments $(t - pt_1)$, where p is any integer and

$$t_1 = \frac{2\pi}{\omega_c} = \frac{2\pi mc}{eH} \qquad (2.9)$$

is the free-electron cyclotron period. Again the δ_+ functions guarantee no states for $E < -E_F + \tfrac{1}{2}\hbar\omega_c$ and the consequent convergence at the lower limit of the integrals involving $\rho(E)$.

In the two cases seen above [(b) of course reduces to (a) when $H = 0$] we can see that, if we are interested in energies close to the Fermi energy ($E \cong 0$) and far away from the bottom of the band, i.e., $|E| \ll E_F$, it is a good approximation to replace in (2.6) and in (B5) the δ_+-functions by simple δ functions. This substitution involves no error in the region of interest but it should be remembered that, when integrating over energies, the lower limit will give rise, in general, to a divergence. The de Haas-van Alphen effect however arises only from the oscillations of the integrals at the upper limit of integration and consequently the approximation is exact if contributions from the lower limit are neglected.

For the rest of this paper we make the following approximations and assumptions in the calculation of G:

(i) All energies are measured from the Fermi energy, i.e.,

$$\zeta = 0,$$

$$\rho(E) = \rho(E - \zeta), \qquad (2.10)$$

$$G(\mathbf{r}_0,\mathbf{r}_0,t) = \exp(i\zeta t/\hbar)G(\mathbf{r}_0,\mathbf{r}_0,t).$$

(ii) Only the two dimensions normal to the magnetic field are considered in G. That is, if H is parallel to the z axis, k_z is a good quantum number. The two-dimensional G, which will be denoted by G_z, is a function of x, y, x_0, y_0, and t, and of k_z as a parameter. In this way (2.5) does not yield the total density of states $\rho(E)$ but only a two-dimensional analogue $\rho_z(E,H,k_z)$ corresponding to a given value k_z of the k-vector parallel to H. The total, three-dimensional, density of states can however be easily obtained by integration

$$\rho(E,H) = \frac{L_3}{2\pi}\int \rho_z(E,H,k_z)dk_z. \qquad (2.11)$$

For the oscillatory components of ρ_z the integral in (2.11) can be simply carried out by means of the so-called Cornu's spiral method[19,20] usually employed in the theory of oscillatory effects in solids.

(iii) $G_z(\mathbf{r},\mathbf{r}_0,t)$ will be approximated by a superposition of wave packets that follow the classical trajectories with well determined phases. These wave packets are formed by electron wave functions in the neighborhood of the Fermi surface and consequently will determine the density of states accurately only for energies close to the Fermi energy; these states are the only ones of interest for the de Haas-van Alphen effect.

From the definition of $G_z(\mathbf{r},\mathbf{r}_0,t)$ and the wave-packet approximation it is evident that except for the contribution to the coefficient of $\delta(t)$, which is equivalent to a constant density of states, only those wave-packets that return to $\mathbf{r}_0$ at a later (or earlier) time give a contribution to $G_z(\mathbf{r}_0,\mathbf{r}_0,t)$. Consequently, for a system which is macroscopically spatially uniform

$$G_z(\mathbf{r}_0,\mathbf{r}_0,t) = \sum_j Y_j \exp\varphi_j\delta(t - t_j), \qquad (2.12)$$

where Y_j and φ_j are the amplitude and phase, respectively, of that wave packet returning to $\mathbf{r}_0$ at a time t_j. In particular φ_j is given by the usual Onsager rules,[1,19] i.e.,

$$\varphi_j = \beta\mathcal{Q}_j(k_z) - \varphi_{j0}, \qquad (2.13)$$

where φ_{j0} is a constant phase, independent of H,

$$\beta = \alpha^{-1} = \frac{\hbar c}{eH}, \qquad (2.14)$$

and $\mathcal{Q}_j(k_z)$ is the area in k space swept by the wave packet j when it returns to $\mathbf{r}_0$ at time t_j. The first term in (2.13) corresponds to 2π times the number of magnetic flux quanta hc/e which the electron has encircled when it returns to $\mathbf{r}_0$.

---

[19] See, for instance, A. B. Pippard, Repts. Progr. Phys. **23**, 176 (1960).

[20] The integral of a function $\exp[i\varphi(x)]$ over x, when φ varies quadratically with x: $\varphi(x) = a + bx^2$ and the interval of integration comprises the origin $x = 0$ and many periods of φ on both sides, is approximately equal to $2x_0 \exp[i(a \pm \pi/4)]$, where $x_0 = \tfrac{1}{2}[\pi|b|]^{-1/2}$ and the plus or minus sign corresponds to positive or negative values of b, respectively. For more details see Ref. 19.

In order to test the validity of the approximations we apply the method to the calculation of the de Haas–van Alphen effect in the free-electron gas,[2] and include later the effect of collisions.[18]

In the case of the free-electron gas, all electrons being at r_0 at $t=0$ return to r_0 at times

$$t_l = lt_1 = \frac{2\pi l}{\omega_c}, \qquad (2.15)$$

where l is any positive or negative integer. The amplitudes Y_l of all the δ functions are in this case identical and equal to the value $2m/\hbar$ determined in (2.6). The phases are given by

$$\varphi_l = l\beta \alpha_1(k_z) - \varphi_{l0}, \qquad (2.16)$$

where

$$\alpha_1(k_z) = \pi(k_F{}^2 - k_z{}^2) = \alpha_1(0) - \pi k_z{}^2. \qquad (2.17)$$

Substitution of all these values in (2.12) yields

$$G_z(r_0, r_0, t)$$

$$= (2m/\hbar) \sum_{l=-\infty}^{\infty} \exp[il\beta \alpha_1(k_z) - i\varphi_{l0}]\delta(t-lt_1), \qquad (2.18)$$

which agrees with the exact equation (B5) if δ is replaced by δ_+ and φ_{l0} is chosen to be equal to $l\pi$. If (2.18) is inserted in (2.5),

$$\rho_z(E,H,k_z)$$

$$= L_1 L_2 \frac{m}{\pi \hbar^2} \sum_{l=-\infty}^{\infty} \exp\{il[\beta \alpha_1(k_z) - \hbar^{-1}Et_1 - \pi]\}, \qquad (2.19)$$

which integrated by means of the Cornu's spiral method over k_z (Ref. 20) according to (2.11) gives for the oscillatory part of the density of states

$$\rho_{osc}(E,H) = \frac{L_1 L_2 L_3}{\pi^2 \hbar^2} \sum_{l=1}^{\infty} (-1)^l (l\beta)^{-1/2}$$

$$\times \cos\{l[\beta \alpha_1(0) - \hbar^{-1}Et_1] - \pi/4\}. \qquad (2.20)$$

Finally, the oscillatory part of the free energy is

$$F_{osc} = 2\pi^{-2} L_1 L_2 L_3 m \sum_{l=1}^{\infty} (-1)^l l^{-5/2} \beta^{-1/2} t_1^{-2}$$

$$\times \frac{X_l}{\sinh X_l} \cos\left[l\beta \alpha_1(0) - \frac{\pi}{4}\right], \qquad (2.21)$$

where

$$X_l = \pi \hbar^{-1} l t_1 k_B T = \frac{2\pi^2 l k_B T}{\hbar \omega_c} = l X_1. \qquad (2.22)$$

Equations (2.21) and (2.22) are identical to the well known result obtained by Landau and Peierls.[2]

The inclusion of collisions into the problem can be accomplished, following Dingle,[18] by assuming that the

wave-packet amplitudes decay in time like

$$M(t) = \exp(-|t|/2\tau), \qquad (2.23)$$

where τ is the usual relaxation time. In this way

$$G_z(r_0, r_0, t) = \frac{2m}{\hbar} \sum_{l=-\infty}^{\infty} \exp[(-|l|t_1/2\tau) + il\beta \alpha_1(k_z) - i\varphi_{l0}]$$

$$\times \delta(t-lt_1), \qquad (2.24)$$

and the final results show a damping of the oscillations by an exponential factor $\exp[-\pi l/\omega_c \tau]$.

3. SYSTEMS WITH COUPLED ORBITS

In the case of magnetic breakdown, the independent semiclassical orbits used in the general formulation thus far become coupled, and the system can be represented by an equivalent network.[7] At each junction (see Fig. 1) a wave arriving through one of the incoming branches with amplitude 1 and zero phase, will leave the junction (a) by continuing on the free-electron trajectory, with amplitude p and phase φ_p or (b) by a Bragg reflected trajectory with amplitude q and phase φ_q. It has been proved[6,7] that

$$p^2 + q^2 = 1, \qquad (3.1)$$

$$\varphi_p - \varphi_q = \pm \tfrac{1}{2}\pi. \qquad (3.2)$$

In addition the probability of continuing along the free-electron trajectory is given by[5,10]

$$P = p^2 = \exp[-H_0/H], \qquad (3.3)$$

where H_0 is a parameter which depends on details of the band structure. For the phases, lacking any detailed knowledge of their value, we follow Pippard[7] and choose $\varphi_p = \tfrac{1}{2}\pi$, $\varphi_q = 0$. This will enable us to compare in the next section our calculation with Pippard's band structure.[7]

The function $G_z(r_0, r_0, t)$ takes now the form

$$G_z(r_0, r_0, t) = \frac{2m}{\hbar} \sum_j C_j M_j R_j \exp(i\varphi_j)\delta(t-t_j), \qquad (3.4)$$

where all the symbols used here will be defined in turn. Under the one label j we have collected all equivalent wave packets, i.e., all those wave packets which return to r_0 at the same time t_j with the same phase φ_j after having followed in their networks similar trajectories, that is, trajectories which become identical after a rotation and/or a translation. The phases φ_j are given by Onsager's rule (2.13).
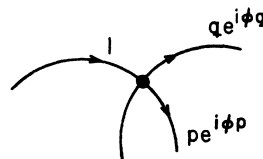

Fig. 1. A junction in a magnetic-breakdown network, showing amplitudes and phases.

If the trajectories pass through n_j junctions and are such that the free-electron path is followed at n_{1j} junctions and the Bragg-reflected path is followed at the remaining n_{2j} junctions,

$$n_{1j}+n_{2j}=n_j, \qquad (3.5)$$

then the factor R_j in (3.4), which we call the magnetic breakdown damping factor, is defined

$$R_j=p^{n_{1i}}q^{n_{2i}}\exp[in_{1j}\varphi_p+in_{2j}\varphi_q], \qquad (3.6)$$

or, following our convention

$$R_j=(ip)^{n_{1j}}q^{n_{2j}}. \qquad (3.7)$$

One would be tempted at this stage to drop the phase factors in (3.6), which, being independent of magnetic field H, can only cause a change in the constant phase of the oscillations. However, as we shall see in a specific example, two different packets may have identical times t_j and phases φ_j but different R_j factors, and in that case interference effects which depend on φ_p and φ_q do arise.

The factor M_j is the usual Dingle scattering factor[18]

$$M_j=\exp[-|t_j|/2\tau]. \qquad (3.8)$$

The factor C_j, called the weight factor, is real and positive and gives the total amplitude of all equivalent packets j. The calculation of C_j involves in general a nontrivial combinatorial problem which needs further clarification. However, in order to make the explanation and discussion less abstract, it is useful at this stage to introduce a specific example and to refer to it. Generalization to other networks is straightforward and will not be done here explicitly.

We consider the hexagonal network used by Pippard[7] and depicted schematically in Fig. 2. It consists in k space of a set of spheres of radius k_F centered at the lattice points of a two-dimensional hexagonal lattice with parameter $|G|$ equal to the magnitude of the first
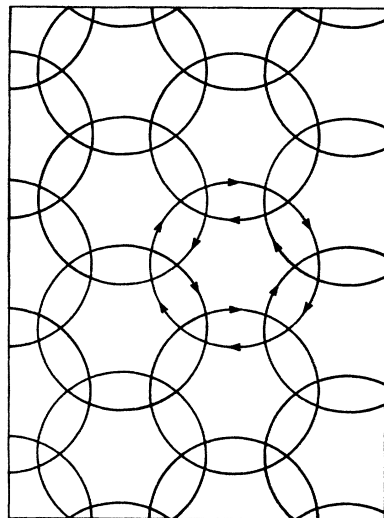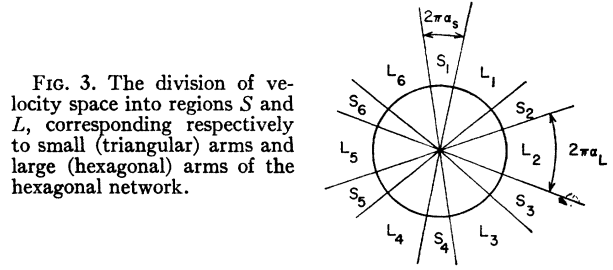

FIG. 2. The hexagonal network in real space.

FIG. 3. The division of velocity space into regions S and L, corresponding respectively to small (triangular) arms and large (hexagonal) arms of the hexagonal network.

reciprocal lattice vector. Figure 2 shows the real-space network which corresponds to a cross section through the centers of the spheres, i.e., at $k_z=0$. This model with different values of k_F and $|G|$ represents very well[10] the actual cases for Mg, Zn, and Be.

If the sense of circulation of the orbits is taken into account, it is seen that the network of Fig. 2 belongs to the two-dimensional space group $p6$,[21] i.e., a group which contains axes of six-, three-, and two-fold symmetry, but contains no mirror planes: the corresponding point group is 6 (or C_6 in the Schoenflies notation).[21]

Since the magnitude of the velocity (or k vector) is a constant throughout the network, a plot of the velocities (Fig. 3) gives a circle divided into twelve arcs. The velocities in each arc correspond to those in one arm of the network and to all other arms equivalent to it under any translation of the space group. The twelve arcs of Fig. 3 can be divided into two sets S and L such that within a set all arcs are equivalent under the rotations of the group. If the angle subtended by each arc S (or L) equals $2\pi\alpha_S$ (or $2\pi\alpha_L$), we call α_S (or α_L) the weight factor of each S (or L) arc, and $6\alpha_S$ (or $6\alpha_L$) the total weight factor of the S (or L) set.

In order to calculate all the quantities involved in (3.4) it is necessary first to draw all possible different trajectories; here we consider as different only those trajectories that cannot be made identical by a completely arbitrary translation and/or one of the rotations of the point group. In Fig. 4 we have drawn twelve possible trajectories. According to our definition orbits (4) and (12) are not different and one of them should be eliminated. On the other hand orbits (7) and (10) are different and both should be included in the calculation.

We make now the following list of parameters for each orbit: (a) the total number of junctions n_j; (b) the number of broken-down junctions n_{1j} and the number of Bragg-reflected junctions n_{2j}: $n_{1j}+n_{2j}=n_j$; (c) the number of small segments n_{Sj} and the number of large segments n_{Lj} comprised in each orbit: $n_{Sj}+n_{Lj}=n_j$; (d) the rotational symmetry of the orbit D_j; this is the number of rotations, including the identity, that transform the orbit into itself; (e) the harmonic order l_j of the orbit, i.e., the total number of times that the wave packet has been at each and every point of the tra-

[21] See, for instance, C. Kittel, *Introduction to Solid State Physics* (John Wiley & Sons, Inc., New York, 1963), p. 16.

TABLE I. Parameters of the orbits appearing in Fig. 4.

Orbit	Number of junctions n_j	Broken down junctions n_{1j}	Bragg-reflected junctions n_{2j}	Number of small segments n_{Sj}	Number of large segments n_{Lj}	Rotational symmetry D_j	Effective mass m_j	Weight C_j	Area in k space $\mathfrak{a}_j(0)$
1	12	12	0	6	6	6	1	1	$\ominus$
2	3	0	3	3	0	3	$3\alpha_S$	$6\alpha_S$	θ
3	6	0	6	0	6	6	$1-6\alpha_S$	$1-6\alpha_S$	χ
4	6	4	2	4	2	2	$\frac{1}{3}+2\alpha_S$	$1+6\alpha_S$	λ
5	12	4	8	6	6	1	1	6	$\chi+2\theta$
6	9	6	3	5	4	1	$\frac{2}{3}+\alpha_S$	$4+6\alpha_S$	$2\lambda-\theta$
7	12	8	4	6	6	2	1	3	$3\lambda-2\theta$
8	12	8	4	6	6	1	1	6	$3\lambda-2\theta$
9	12	6	6	6	6	3	1	2	$3\lambda-2\theta$
10	12	8	4	6	6	2	1	3	$3\lambda-2\theta$
11	12	4	8	6	6	2	1	3	$\chi+2\theta$

jectory; (f) the extremal area of the orbit in k space $\mathfrak{a}_j(0)$.[22] Of all numbers in the list, n_{1j}, n_{2j}, n_{Sj}, and n_{Lj} are non-negative; l_j, n_j, and D_j are positive and $\mathfrak{a}_j(0)$ can take any value, positive or negative.

With all these parameters written down (see Table I and Fig. 4 for various examples) we calculate

(A) the effective-mass parameter

$$m_j = n_{Sj}\alpha_S + n_{Lj}\alpha_L, \tag{3.9}$$

where α_S and α_L are the weight factors of the small and large arcs, respectively, (Fig. 3); (B) the times t_j needed by the wave packets to return to r_0:

$$t_j = \pm m_j t_1, \tag{3.10}$$

where t_1 is the free-electron cyclotron period (2.9); (C) the phases φ_j at the extremum

$$\varphi_j = \pm\beta\mathfrak{a}_j(0)\mp\varphi_{j0}, \tag{3.11}$$

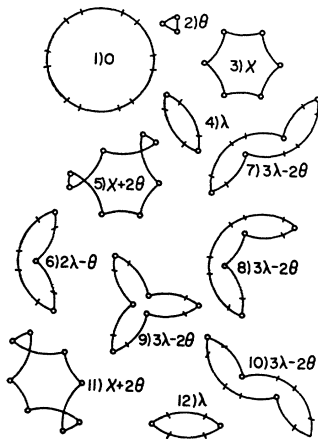where β is defined in (2.14) and the signs are chosen so

FIG. 4. Some possible orbits in the hexagonal network.

that the upper (lower) sign in (3.11) corresponds to the upper (lower) sign in (3.10); (D) the magnetic-breakdown damping factor R_j given by (3.6) [or (3.7)]; (E) the Dingle scattering factor M_j given by (3.8) and (3.10); (F) the weight factor C_j, given by[22a]

$$C_j = \frac{6m_j}{D_j l_j}. \tag{3.12}$$

This completes the information required to write G_z in (3.4). However, when performing the integral (2.11) over k_z, it is necessary to know the variation of $\mathfrak{a}_j(k_z)$ with k_z. This[20] is only necessary close to the extremum $k_z=0$, where it can be approximated by

$$\mathfrak{a}_j(k_z) = \mathfrak{a}_j(0) + \frac{\partial\mathfrak{a}_j}{\partial(k_j^2)}k_z^2. \tag{3.13}$$

We can then calculate (G) the coefficient of the quadratic variation of area $\mathfrak{a}_j(k_z)$ at the extremum; a straightforward calculation gives

$$\frac{\partial\mathfrak{a}_j}{\partial(k_z^2)} = -\pi m_j. \tag{3.14}$$

When all these values are replaced in (3.4), (2.5), (2.11), and (2.2), the oscillatory part of the free energy F_{osc} is given by

$$F_{osc} = 2\pi^{-2}L_1L_2L_3 m \sum_j \frac{6}{D_j l_j}\beta^{-1/2}m_j^{-3/2}t_1^{-2}(ip)^{n_{1j}}q^{n_{2j}}$$

$$\times\exp[-m_j t_1/2\tau]\frac{X_j}{\sinh X_j}\cos\left[\beta\mathfrak{a}_j(0) - \varphi_{j0}-\frac{\pi}{4}\right], \tag{3.15}$$

---

[22] In measuring the orbit area, the orbits or those closed parts of an orbit which are of the electron type are considered positive, while orbits or closed parts of orbits which are of the hole type are negative. In Table I and Fig. 4, $\ominus$, θ, and λ are positive while χ is negative.

[22a] *Note added in proof.* C_j is the product of the effective mass of the fundamental frequency, (m_j/l_j), and the number of equivalent, nonidentical orbits which contribute to j, $(6/D_j)$.

where t_1 is the free-electron cyclotron period,

$$X_j = m_j X_1 = m_j \frac{2\pi^2 k_B T}{\hbar \omega_c}, \qquad (3.16)$$

and ω_c is the free-electron cyclotron frequency.

Formula (3.15) gives the final result of this calculation. In the next section we apply it to the specific case of magnesium and we also compare the resulting density of state with a numerical calculation of $\rho(E,H)$ for constant H as a function of E obtained by an extension of Pippard's band structure.[7]

4. APPLICATION TO MAGNESIUM

In the case of Mg[23]

$k_F = 0.7274$ atomic units (radius of Fermi sphere);

$|G| = 1.2040$ atomic units (distance between centers in the network).

These result in the following parameters for the hexagonal network:

$$\alpha_S \cong 5/216 = 0.0231,$$

$$\alpha_L \cong 31/216 = 0.1435,$$

$O =$ Area of circle $= 1.66$ a.u. [Fig. 4. (1)],

$\theta =$ Area of triangle $= 6.49 \times 10^{-3}$ a.u. [Fig. 4. (2)],

$X =$ Area of hexagon $= -8.63 \times 10^{-1}$ a.u. [Fig. 4. (3)],

$\lambda =$ Area of lens $= 1.39 \times 10^{-1}$ a.u. [Fig. 4. (4)].

The constant

$$\gamma = \alpha_L/\alpha_S = 6.2$$

corresponds exactly to one of the values chosen by Pippard[7] for the calculation of the band structure of an hexagonal system of coupled orbits [Fig. 8 of Ref. 7].

We have calculated the amplitude of some of the important oscillatory components of the free energy (3.15) for this case. We have estimated[10]

$$H_0 \cong 5.8 \text{ kG}$$

as the value for the breakdown field (3.3) and we have chosen a temperature $T = 1°K$, for which

$$X_j = \frac{147 m_j}{H(\text{kG})}.$$

The various orbits for which the amplitude was computed are described in Table II. The calculated amplitudes (3.15) for fields up to 150 kG are shown in Fig. 5.

The following features are worth mentioning:

(a) The small triangular orbit θ is dominant throughout the studied range of magnetic fields; although at

TABLE II. Parameters of some important orbits in magnesium.

Area $\alpha_j(0)$	Rotational symmetry D_j	Harmonic order l_j	Effective mass m_j	n_{1j}	n_{2j}	Number in Fig. 4
O	6	1	1.000	12	0	(1)
$2O$	6	2	2.000	24	0	⋯
$3O$	6	3	3.000	36	0	⋯
$4O$	6	4	4.000	48	0	⋯
θ	3	1	0.069	0	3	(2)
2θ	3	2	0.139	0	6	⋯
3θ	3	3	0.208	0	9	⋯
X	6	1	0.861	0	6	(3)
$2X$	6	2	1.722	0	12	⋯
λ	2	1	0.380	4	2	(4)
2λ	2	2	0.759	8	4	⋯
$\lambda+\theta$	1	1	0.449	4	5	⋯
$2\lambda-\theta$	1	1	0.690	6	3	(6)
$2O-\lambda$	2	1	1.620	16	2	⋯

150 kG the factor q^3 is rather small ($\sim 1.8 \times 10^{-3}$), the small effective mass still makes the period a predominant one.

(b) The harmonic content of θ decreases strongly as the magnetic field increases; this can be seen in the amplitudes of 2θ and 3θ, and is the opposite to the usual behavior of de Haas–van Alphen line-shapes.

(c) The circular orbit O and its higher harmonics become most important at high fields; the harmonic content in this case increases more strongly than in a normal oscillation.

(d) The hexagonal orbit X has always an extremely small amplitude, which explains why, although geometric considerations make it a favorable one to observe, it has not been detected experimentally.[12] In this case the rather large mass $m_j \cong 0.86$ and the very large magnetic-breakdown damping factor q^6 result in the small amplitude throughout.

The abundance of periods as well as the irregular magnetic field dependence of the amplitudes have been observed experimentally in Zn [3,16,24] and Mg.[17] In the case of Zn, Pippard[7] has derived a result practically identical to ours for the small triangular orbits θ, which compares very well with the measurements of Dhillon and Shoenberg.[3] Further quantitative comparison between experiment and the present theory should be of great interest and it will undoubtedly be made when the experimental data become available.

We have performed one more direct test of our theory by comparing our two dimensional density of states $\rho_z(E,H)$ considered as a function of E at a constant H and q, with that obtained numerically from the magnetic band structure calculation of Pippard.[7]

Our calculation in Sec. 3 yields for the oscillatory

[23] L. M. Falicov, Phil. Trans. Roy. Soc. London A255, 55 (1962).

[24] J. R. Lawson and W. L. Gordon, in Proceedings of the IXth International Conference on Low Temperature Physics, Columbus, Ohio, 1964 (Plenum Press, New York, 1965), p. 854.
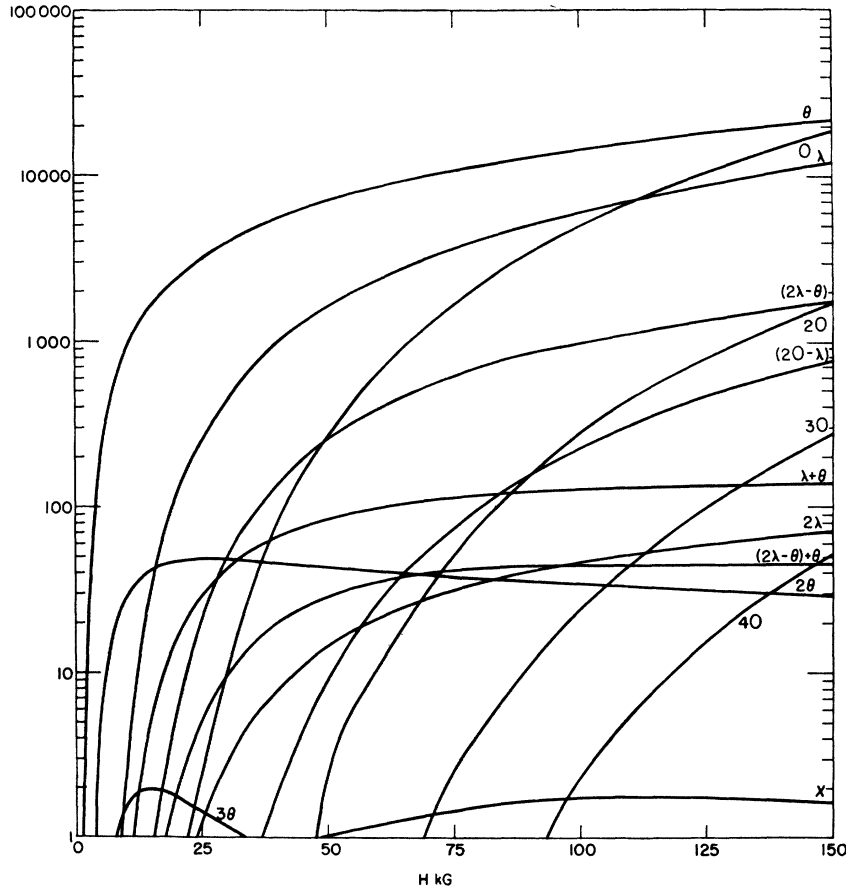
FIG. 5. The magnetic-field dependence of the amplitude of the oscillatory free energy for various periods. The parameters are chosen to resemble magnesium at a temperature $T = 1°K$. The amplitude scale is in arbitrary units and the symbols for the orbits are shown in Fig. 4.

part of $\rho_z(E,H)$

$$\rho_z(E,H) = L_1 L_2 \frac{m}{\pi\hbar^2} \sum_j \frac{6m_j}{D_j l_j} (ip)^{n_{1j}} q^{n_{2j}} \exp[-m_j t_1/2\tau]$$

$$\times \cos[\beta\alpha_j(0) - \varphi_{j0} - \hbar^{-1} E m_j t_1]. \quad (4.1)$$

As a function of E, $\rho_z(E,H)$ is a multiply periodic function, with frequencies proportional to m_j. In order to compare our calculation with Pippard's, we consider the amplitudes of a given frequency; we choose $\tau \to \infty$ and obtain

$$\rho(m_o) \propto \sum_{\substack{j \\ m_j = m_o}} \frac{6m_o}{D_j l_j} (ip)^{n_{1j}} q^{n_{2j}}, \quad (4.2)$$

where, for simplicity and following Pippard, all phases are such that at the chosen value of magnetic field

$$\beta\alpha_j(0) - \varphi_{j0} = 2\pi n. \quad (4.3)$$

The dependence of (4.2) on q can now be checked. The numerical calculations of $\rho(m_o)$ from Pippard's band structure are described in detail in Appendix C. The result for the q dependence of $\rho(m_o = 1)$ is shown in Fig. 6 in the full line labeled "Total for Free Electron Mass." This curve shows an unexpected behavior, with

a change in sign as well as several inflexion points, and it is evident that it can arise from (4.2) only if several orbits j with $m_j = 1$ contribute. Table III shows an analysis of all possible nine orbits which have a free-electron effective mass; they correspond to three essentially different de Haas–van Alphen periods with areas Θ, $(3\lambda - 2\theta)$, and $(\chi + 2\theta)$. The q dependence of the amplitude for each area is shown in Fig. 6, and it is seen that they add up exactly to the numerically com-

TABLE III. Parameters of all orbits with the free-electron mass. $m_j = 1$; $n_j = 12$; $n_{Sj} = n_{Lj} = 6$.

Area $\alpha_j(0)$	D_j	n_{1j}	n_{2j}	C_j	Number in Fig. 4
Θ	6	12	0	1	(1)
$3\lambda - 2\theta$	3	6	6	2	(9)
$3\lambda - 2\theta$	2	8	4	3	(7)
$3\lambda - 2\theta$	2	8	4	3	(10)
$3\lambda - 2\theta$	1	8	4	6	(8)
$\chi + 2\theta$	2	4	8	3	(11)
$\chi + 2\theta$	1	4	8	6	(5)
$\chi + 2\theta^a$	1	4	8	6	...
$\chi + 2\theta^b$	1	2	10	6	...

a Corresponds to one hexagonal orbit and two triangular orbits in neighboring corners.
b Corresponds to one hexagonal orbit and twice the same triangular orbit.
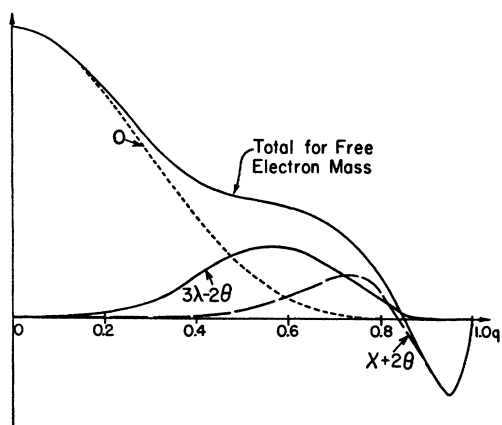
FIG. 6. The Fourier component of the density of states $\rho_z(E,H)$ for the free-electron mass $m_0 = 1$ as a function of the parameter q. The curve labeled "total for free-electron mass" is the result of the numerical calculation based on Pippard's band structure (Ref. 7); the three partial components ϑ, $(3\lambda - 2\theta)$, and $(\chi + 2\theta)$ are the results of the present calculation, and they add up to the value of the first curve.

puted curve within the accuracy of the numerical calculation.

It is interesting to note that for the $(3\lambda - 2\theta)$ area as well as for $(\chi + 2\theta)$, two types of q dependence appear, i.e.,

$$12p^8q^4 - 2p^6q^6, \quad \text{for} \quad (3\lambda - 2\theta);$$

$$15p^4q^8 - 6p^2q^{10}, \quad \text{for} \quad (\chi + 2\theta).$$

The minus signs are due to the imaginary factors in front of the breakdown amplitude (ip); this imaginary factor gives rise, as expected, to interference effects. For instance the amplitude of the period arising from $(\chi + 2\theta)$, if it could be observed experimentally, should go through zero for $q \cong 0.85$, $H \cong 0.8H_0 \cong 4.8$ kG.

The agreement between the two calculations is very satisfactory and is certainly one further argument which justifies the validity of our wave-packet assumption in the calculation of G_z.

5. CONCLUSIONS

We have presented a method of calculating the amplitude of the de Haas–van Alphen oscillations in the presence of magnetic breakdown. The main result of the theory is given by formula (3.15). It has been shown that the method has the following features:

(a) It is based on an exact Green's function formulation.

(b) It has been approximated by a semiclassical approach in which the relevant part of the Green's function is expressed as a superposition of wave packets with well defined phases and amplitudes.

(c) The approximations involve no error in the case of the free electron gas.

(d) It gives the right kind of magnetic field as well

as temperature-dependence of the effect which agrees very well with previous partial theoretical results[7] as well as experimental results in Zn^2 and qualitative[12] as well as preliminary quantitative[17] data for Mg.

(e) It gives the right dependence on the magnetic breakdown parameters p and q for the oscillatory part of the density of states which arises from closed orbits.

(f) It does not include spurious oscillations with magnetic field; i.e., only those oscillations arising from actual orbits which satisfy Onsager's rule give a contribution to the magnetic field dependence of the density of states.

ACKNOWLEDGMENTS

APPENDIX A

If $\{\varphi_n\}$ are the eigenfunctions of the Hamiltonian $\mathcal{H}$ with eigenvalues $\{E_n\}$

$$\mathcal{H}\varphi_n = E_n\varphi_n, \tag{A1}$$

it can be seen, by direct substitution and the use of orthogonality and completeness properties of $\{\varphi_n\}$, that

$$G(\mathbf{r},\mathbf{r}_0,t) \equiv \sum_n \varphi_n^*(\mathbf{r}_0)\varphi_n(\mathbf{r}) \exp[-iE_nt/\hbar] \tag{A2}$$

satisfies Eqs. (2.3)–(2.4). The density of states $\rho(E)$ is defined by

$$\rho(E) \equiv \sum_n \delta(E - E_n)$$

$$= \sum_n \frac{1}{2\pi\hbar} \int_{-\infty}^{\infty} \exp[i(E - E_n)t/\hbar]dt. \tag{A3}$$

Equation (2.5) is now proved by multiplying (A2) by $\exp[iEt/\hbar]$, putting $\mathbf{r} = \mathbf{r}_0$ integrating over space and time and making use of the normalization condition of $\{\varphi_n\}$

$$\int \varphi_n^*(\mathbf{r}_0)\varphi_n(\mathbf{r}_0)d\mathbf{r}_0 = 1. \tag{A4}$$

APPENDIX B

For a free-electron gas in two dimensions (x,y) with a magnetic field H in the z direction, if we choose the asymmetric gauge

$$A = (0, Hx), \tag{B1}$$

the one-electron wave functions are given by[2]

$$\varphi_{lk} = \alpha^{1/4}(L_2)^{-1/2} \exp(iky) \exp[-(\alpha x - k)^2/2\alpha]$$
$$\times H_l\left(\frac{\alpha x - k}{\sqrt{\alpha}}\right), \tag{B2}$$

where

$$\alpha = (eH)/(\hbar c) \tag{B3}$$

and H_l is a Hermite polynomial of order l normalized to unity. The energy eigenvalues are

$$E_{lk} = (l+\tfrac{1}{2})\frac{\hbar eH}{mc} - E_F = (l+\tfrac{1}{2})\hbar\omega_c - E_F. \tag{B4}$$

Substitution of (B2) and (B4) into (A2) and integration over x and y as well as summation over k yield

$$G(\mathbf{r}_0, \mathbf{r}_0, t) = \frac{\alpha}{\pi}\sum_{l=0}^{\infty} \exp[-iE_{lk}t/\hbar]$$

$$= \frac{2m}{\hbar}\exp\left[i\left(\frac{E_F}{\hbar} - \frac{\omega_c}{2}\right)t\right]\sum_{p=-\infty}^{\infty} \delta_+(t - pt_1), \tag{B5}$$

where t_1 is the cyclotron period. It should be noted that in obtaining (B5) the summation over k has been replaced by an integration

$$\sum_k \Rightarrow \frac{L_2}{2\pi}\int_{-\infty}^{\infty} \cdots dk, \tag{B6}$$

and in turn this can be replaced by an integral over the argument of the Hermite polynomials.

APPENDIX C

Pippard's expression for the eigenvalues of the system of coupled orbits [Eqs. (35) and (41) of Ref. 7], can be greatly simplified if one restricts oneself to special values of the propagation vector in the magnetic zone. In particular the points Γ (center of the hexagonal zone), K (corner of the zone), and M (midpoint of the side of the hexagon) are particularly convenient. The energy is given by the roots of the following equations:
At Γ $\omega_1 = \omega_2 = \omega_3 = 0$

$$\cos[(\gamma+1)\tfrac{1}{2}x_\Gamma] - q\cos[(\gamma-1)\tfrac{1}{2}x_\Gamma] = 0, \tag{C1}$$

$$\cos[(\gamma+1)\tfrac{1}{2}x_\Gamma - \tfrac{2}{3}\pi] - q\cos[(\gamma-1)\tfrac{1}{2}x_\Gamma] = 0, \tag{C2}$$

$$\cos[(\gamma+1)\tfrac{1}{2}x_\Gamma - \tfrac{4}{3}\pi] - q\cos[(\gamma-1)\tfrac{1}{2}x_\Gamma] = 0, \tag{C3}$$

$$\sin[(\gamma+1)\tfrac{1}{2}x_\Gamma] - q\sin[(\gamma-1)\tfrac{1}{2}x_\Gamma] = 0, \tag{C4}$$

$$\sin[(\gamma+1)\tfrac{1}{2}x_\Gamma - \tfrac{2}{3}\pi] - q\sin[(\gamma-1)\tfrac{1}{2}x_\Gamma] = 0, \tag{C5}$$

$$\sin[(\gamma+1)\tfrac{1}{2}x_\Gamma - \tfrac{4}{3}\pi] - q\sin[(\gamma-1)\tfrac{1}{2}x_\Gamma] = 0. \tag{C6}$$

At K $\omega_1 = \omega_2 = -2\omega_3 = 2\pi/3$,

$$\sin[(\gamma+1)x_K] + q\sin[\gamma x_K]$$
$$+ q^2\sin[(\gamma-1)x_K] = 0, \tag{C7}$$

$$\sin[(\gamma+1)x_K - \tfrac{2}{3}\pi] + q\sin[\gamma x_K - \tfrac{4}{3}\pi]$$
$$+ q^2\sin[(\gamma-1)x_K] = 0, \tag{C8}$$

$$\sin[(\gamma+1)x_K - \tfrac{4}{3}\pi] + q\sin[\gamma x_K - \tfrac{2}{3}\pi]$$
$$+ q^2\sin[(\gamma-1)x_K] = 0. \tag{C9}$$

At M $\omega_1 = \pi$ $\omega_2 = 0$ $\omega_3 = -\pi$,

$$\sin[(\gamma+1)\tfrac{3}{2}x_M] + (1-q^2)q\sin[(\gamma-1)\tfrac{1}{2}x_M]$$
$$- q^3\sin[(\gamma-1)\tfrac{3}{2}x_M] = 0, \tag{C10}$$

$$\cos[(\gamma+1)\tfrac{3}{2}x_M] - (1-q^2)q\cos[(\gamma-1)\tfrac{1}{2}x_M]$$
$$- q^3\cos[(\gamma-1)\tfrac{3}{2}x_M] = 0. \tag{C11}$$

In these equations $\gamma = 6.2$, q is given by (3.1), (3.3), and x is related to the energy by

$$x = \frac{\pi E}{3(1+\gamma)\hbar\omega_c}. \tag{C12}$$

Equations (C1) to (C11) are periodic in x, with a period $\Delta x = 10\pi$. A change in energy equal to the free-electron cyclotron energy corresponds to a change

$$\delta x = \frac{\pi}{3(1+\gamma)} = \frac{10\pi}{216},$$

i.e., it is related to a frequency which is the 216th harmonic of the fundamental frequency.[25]

Due to the tight binding character of the energy curves,[7] the points Γ and K correspond one to the bottom and the other to the top of the magnetic bands; x_M always lies between a x_Γ and a x_K point and in addition the bands may touch, but never overlap. The density of states was calculated by assuming that the expression $C(x)$ [Eq. (41) of Ref. 7] given by Pippard could be linearly interpolated between two neighboring x_Γ and x_M values, and between two neighboring x_M and x_K values, i.e.,

$$C(x) = 3 - 4\frac{x - x_\Gamma}{x_M - x_\Gamma}, \qquad x \text{ between } x_\Gamma \text{ and } x_M,$$
$$\tag{C13}$$
$$= -1 - 0.5\frac{x - x_M}{x_K - x_M}, \qquad x \text{ between } x_M \text{ and } x_K.$$

---

[25] In the same context, the harmonic order of any orbit j is given by $n = 216m_j$. In particular n takes the values of 15 for θ, 82 for λ and 186 for χ. Although only the calculation for $n = 216$ is reported here, all harmonic orders up to $n \cong 900$ were calculated and good agreement was found throughout.

The density of states was finally approximated by

$$\rho_z(C) = 10.20 - 4.16C + 0.765C^2, \qquad -0.5 < C < 3,$$
$$\quad\;\; = -1.80 - 28.16C + 0.765C^2, \quad -1 < C < -0.5,$$
$$\quad\;\; = 52.80 - 24C, \qquad\qquad\qquad -1.5 < C < -1.$$

(C14)

Equation (C14) is a good approximation to the two-dimensional density of states for an hexagonal tight-binding system. It has been arbitrarily normalized such that

$$\int_{-1.5}^{+3} \rho_z(C)dC = 45.70.$$

(C15)

The quantities of interest are the amplitudes of the Fourier components of this two-dimensional density of states, i.e.,

$$\rho_n(q) = \frac{1}{10\pi} \int_{-5\pi}^{5\pi} \rho_z(x) \exp[-inx/5]dx$$

$$= \frac{1}{5\pi} \int_0^{5\pi} \rho_z(C)\frac{dC}{dx} \cos[nx/5]dx.$$

(C16)

In particular, for the free electron mass, $m_0 = 1$, $n = 216$.

The numerical calculations involved in the determination of the energy eigenvalues (C1) to (C11) as well as the integrations (C16) for the Fourier components ρ_n were carried out in the IBM 7094-7044 complex of the University of Chicago Computation Center.

Radiation from Thick Silver Foils Bombarded by Grazing-Incidence Electrons*

G. E. Jones,[†] L. S. Cram,[‡] and E. T. Arakawa
Health Physics Division, Oak Ridge National Laboratory, Oak Ridge, Tennessee
(Received 14 February 1966)

Silver foils several thousand angstroms in thickness were bombarded by electrons at grazing incidence. A peak was observed at approximately 3550 Å in the optical emission spectrum. For an angle of incidence of 89° from the foil normal, the peak intensity was approximately ten times as great as that of previously observed intensities of transition radiation at 3300Å from silver foils bombarded with normally incident electrons. The intensity was found to be directly proportional to the electron energy from 40 to 80 keV, and showed a marked dependence on the quality of the foil surface. The results are in agreement with the findings of Boersch *et al.*

INTRODUCTION

IT was shown by Ritchie[1] that in addition to collective oscillations by the bulk electrons in a conductor, there should exist plasma oscillations on the conductor surface. Ferrell[2] predicted that bulk plasma oscillations induced by charged particle excitation should decay by the emission of monochromatic photons at the plasma frequency. Since Ferrell's prediction, many investigators[3] have searched for plasma radiation. Most of these investigators have bombarded metal foils with normally incident electrons and have interpreted the emission spectra in terms of the decay of volume plasmons. Recently Boersch *et al.*[4] bombarded silver foils with 30-keV electrons at grazing incidence and found an intense peak at 3500 Å, which was thought to be due to the decay of surface plasma oscillations. However, Ferrell's model of a conductor bounded by a plane surface forbids emission by the decay of surface plasma oscillations.

This paper presents the results of a further attempt to determine whether or not surface plasma oscillations decay by emission of electromagnetic radiation. Thick silver foils were bombarded by grazing-incidence electrons. The emission spectrum was studied as a function of the angle of incidence of the electron beam, the electron energy, and the quality of the foil surface.

EXPERIMENTAL

The techniques used in measuring the optical emission from electron-bombarded foils have been described

[1] R. H. Ritchie, Phys. Rev. **106**, 874 (1957).
[2] R. A. Ferrell, Phys. Rev. **111**, 1214 (1958).
[3] W. Steinmann, Phys. Rev. Letters **5**, 470 (1960); Z. Physik **163**, 92 (1961); R. W. Brown, P. Wessel, and E. P. Trounson, Phys. Rev. Letters **5**, 472 (1960); A. L. Frank, E. T. Arakawa, and R. D. Birkhoff, Phys. Rev. **176**, 1947 (1962).
[4] H. Boersch, P. Dobberstein, D. Fritzsche, and G. Sauerbrey, Z. Physik **187**, 97 (1965).